The response of the North Atlantic bloom to NAO forcing

Ken-ichi Mizoguchi[1], Denise L. Worthen[2], Sirpa Häkkinen[3] and Watson W. Gregg[3]

May 20, 2004

(1) GEST, University of Maryland at Baltimore County, Baltimore, Maryland

(2) Science Systems and Applications, Inc, 10210 Greenbelt Rd Suite 600, Lanham, Maryland

(3) NASA/Goddard Space Flight Center, Greenbelt, Maryland

Corresponding author e-mail: sirpa.hakkinen@nasa.gov

Abstract

Results from the climatologically forced coupled ice/ocean/biogeochemical model that covers the Arctic and North Atlantic Oceans are presented and compared to the chlorophyll fields of satellite-derived ocean color measurements. Biogeochemical processes in the model are determined from the interactions among four phytoplankton functional groups (diatoms, chlorophytes, cyanobacteria and coccolithophores) and four nutrients (nitrate, ammonium, silicate and dissolved iron). The model simulates the general large-scale pattern in April, May and June, when compared to both satellite-derived and *in situ* observations.

The subpolar North Atlantic was cool in the 1980s and warm in the latter 1990s, corresponding to the CZCS and SeaWiFS satellite observing periods, respectively. The oceanographic conditions during these periods resemble the typical subpolar upper ocean response to the NAO+ and NAO- phases, respectively. Thus, we use the atmospheric forcing composites from the two NAO phases to simulate the variability of the mid-ocean bloom during the satellite observing periods. The model results show that when the subpolar North Atlantic is cool, the NAO+ case, more nutrients are available in early spring than when the North Atlantic is warm, the NAO- case. However, the NAO+ simulation produces a later bloom than the NAO- simulation. This difference in the bloom times is also identified in SeaWiFS and CZCS satellite measurements. In the model results, we can trace the difference to the early diatom bloom due to a warmer upper ocean. The higher nutrient abundance in the NAO+ case did not provide larger total production than in the NAO- case, instead the two cases had a comparable area averaged amplitude. This leads us to conclude that in the subpolar North Atlantic, the timing of the spring phytoplankton bloom depends on surface temperature and the magnitude of the bloom is not significantly impacted by the nutrient abundance.

1. Introduction

Ocean phytoplankton are responsible for approximately half of the global biospheric net primary production (Behrenfeld et al., 2001). Thus, the sequestration and export of carbon by ocean phytoplankton (the biological carbon pump) is a major component in the global carbon cycle. Variations in ocean primary production as a result of changes in oceanic or atmospheric conditions can have important implications for regulating the sequestration of atmospheric CO_2.

The northern North Atlantic Ocean is a suitable region to explore the linkages between variations in climate regimes and the accompanying ecosystem response for two reasons. First, the subpolar North Atlantic is a region characterized by a large and intense spring phytoplankton bloom. Secondly, the North Atlantic Ocean has a coherent link to a natural atmospheric mode, the North Atlantic Oscillation (NAO) at interannual and decadal time scales (Cayan 1992). This mode is characterized by the fluctuations of a north-south dipole, co-varying with a tripole pattern of sea surface temperature anomalies (SSTA), which is an upper ocean response to the NAO (Deser and Blackmon, 1993). Inside the Labrador Sea, NAO forcing is linked to convective activity (Marshall and Schott, 1999), which exhibits distinct decadal periods of absence and intensification (Dickson et al., 1996).

Various observational (in situ) and modeling studies have addressed the relationship between ocean productivity and meteorological conditions. Modeling studies have shown that different physical mechanisms control the biological responses in the subtropical and subpolar regions of the North Atlantic Ocean: Dutkiewicz et al. (2001) and Follows and Dutkiewicz (2002) conducted numerical studies to examine the interannual variability in springtime chlorophyll concentrations as a response to surface forcing changes. In the subtropics, spring mixing leads to enhanced chlorophyll concentrations whereas in the subpolar gyre, strong mixing

leads to lower phytoplankton abundances. These authors showed that chlorophyll abundance in the subpolar gyre has a relationship to the variation in the surface heat flux. These authors did not find a consistent response to the local NAO forcing, a finding, which was also presented in Barton et al. (2003) based on Continuous Plankton Recorder observations. However, several other observational studies on the phytoplankton and zooplankton abundance have found linkages to NAO. Dickson et al (1988) found that the decline in the phytoplankton around British Isles from the 1950s through the 1980s is associated with strong Azores High, which is the southern center of NAO. Conversi et al. (2001) found that interannual fluctuations of *Calanus finmarchicus* abundance in the Gulf of Maine between 1961 and 1991 were positively correlated with the NAO index. In a study of observed phytoplankton trends between 1960 and 1995, Reid et al. (1998) and Edwards et al. (2001) highlighted the importance of surface temperature and the influence of NAO.

Remotely sensed ocean color data provide another source of global ocean chlorophyll observations. The Coastal Zone Color Scanner (CZCS; 1978-1986) and the Sea-Viewing Wide Field of View Sensor (SeaWiFS; 1997-present) provide a global dataset for investigating large-scale chlorophyll variability. Gregg and Conkright (2002) used remotely sensed ocean chlorophyll data to show that the summer phytoplankton biomass in the North Atlantic has dropped by 14 percent from the mid-80s to the present. The reduction of chlorophyll biomass observed in the satellite record was found to be largely due to a decrease in the central and northern portions of the North Atlantic basin. In addition, the spring bloom peak in the northern North Atlantic was higher in the present decade and diminished more quickly, indicating a change in the bloom dynamics between the SeaWiFS and the CZCS period, a result also presented by Gregg (2002).

The observational periods of CZCS and SeaWiFS have occurred during different regimes of the NAO, although as measured by the NAO index this association is not robust. During CZCS years, the NAO index was positive in seven out of nine winters (Nov-Apr) (Fig. 1a). The NAO index became strongly negative in the winter of 1996, just prior to the beginning of the SeaWiFS observing period but has since steadily climbed, reaching positive values by the winter of 1999. However, very warm surface conditions usually associated with negative NAO conditions have persisted in the subpolar North Atlantic during the SeaWiFS period. The warming trend is evidenced by the SST variability as an area average in the northern North Atlantic (Fig. 1b) and SST difference between the CZCS and SeaWiFS period (Fig. 1c). The anomalously warm upper ocean conditions during the most recent positive NAO years have occurred because of the eastward shift in the NAO northern center. As a result, the strong heat loss typical of the NAO+ conditions in the subpolar gyre has failed to materialize and surface temperatures have remained warm and more typical of NAO- conditions (Häkkinen and Rhines, 2004). Since the upper ocean conditions during the SeaWiFS period resemble the ocean response to negative NAO, the NAO index provides a simple framework for differentiating the climatic conditions in the subpolar North Atlantic during the CZCS and SeaWiFS observing periods.

Considering the ocean chlorophyll trend in the North Atlantic and the changes in the character of the spring bloom, a natural question arises: are the decadal changes in the chlorophyll biomass part of a long-term trend or are they a response to the variability of the upper ocean at the decadal time scale? To investigate this question, three numerical experiments are carried out in this study. A coupled ice/ocean/biogeochemical model of the Arctic and North Atlantic Ocean is forced with the long-term mean atmospheric forcing as well as with atmospheric forcing composited from the high (NAO+) and low (NAO-) phases of NAO. As

noted in Gregg and Conkright (2002), the largest chlorophyll changes between CZCS and SeaWiFS are found in the subpolar North Atlantic where the bloom is located in the mid-ocean in isolation from boundary forcing (both rivers and river nutrients). Thus, we limit our discussion to chlorophyll changes in the subpolar gyre. The experiments are designed to attempt to simulate the May bloom identified during SeaWiFS (negative NAO-like conditions) and the June bloom during CZCS (positive NAO-like conditions). Our results indicate that the timing of the bloom is sensitive to surface temperature conditions in spring and that nutrient availability is less important factor in the subpolar North Atlantic.

The model description is in section 2, the results are shown comparing to other observations in section 3. A summary and discussion follows in the section 4.

2 Model Description

2.1 Coupled ice/ocean model

The ice/ocean model is a fully prognostic three-dimensional primitive equation model based on the Princeton Ocean Model (POM). It is hydrostatic and Boussinesq and uses the sigma-coordinate system as described by Blumberg and Mellor (1987) with a modified scalar advection scheme to avoid overshooting at sharp fronts (Mauritzen and Häkkinen, 1997). The model domain extends from the Bering Strait to 15°S with a horizontal resolution of 7/10° in longitude and 9/10° in latitude. There are a total of 20 sigma-levels in the vertical with a high density of levels in the first 50 meters to resolve the mixed-layer dynamics. The level 2.5 turbulence closure scheme of Mellor and Yamada, (1982) is used to determine the vertical mixing coefficients for momentum and scalar variables. When vertical instabilities occur, convection is parameterized as vertical mixing at a large diffusion coefficient. A dynamic-

thermodynamic ice model is coupled to the ocean model via interfacial stresses and salinity and heat fluxes through the ice-water interface. The ice model uses a generalized viscous rheology, as discussed by Häkkinen and Mellor (1992).

The ice/ocean model is forced for 20 years with atmospheric climatological data from National Center for Environmental Prediction (NCEP) reanalysis (1948-2002). The climatological NCEP data used are wind stress, wind speed, air temperature and specific humidity. The climatological cloudiness, P-E and river runoff data used are described in Häkkinen (2002). The surface boundary condition for salinity uses virtual flux of salt, i.e., (P-E)*SSS. Similarly the river runoff represents a virtual flux of salt. The rivers supply no nutrients.

The bulk formulation is adopted for the heat exchange wherein the heat fluxes are a function of the oceanic surface quantities. A heat exchange with coefficient of 1.3×10^{-3} is used regardless of air-ocean stability conditions. The surface mixing ratio is computed from the model generated surface temperature with 98% saturation. The model SST is also used in the upward longwave radiation. The climatology run was initialized with the annual average hydrographic climatology of Levitus et al. (1994). The output from the end of the 20th year is used as an initial field for the coupled ice/ocean/biological model. The internal time step of ice/ocean model is 18 minutes and the output at every time step is one-way coupled to the biogeochemical model.

2.2 Biogeochemical model

The biogeochemical model of Gregg et al. (2003); Gregg (2002) was coupled to the ice-ocean model described above. The biogeochemical model contains four phytoplankton functional groups (diatoms, chlorophytes, cyanobacteria, and coccolithophores), four nutrients (nitrate, ammonium, silica, and dissolved iron), a single herbivore group and two detrital pools.

The horizontal and vertical distributions of the biological components are determined by advective and mixing processes in the ocean model as well as by local growth and decay processes. Full details of the parameterizations of these processes can be found in the references cited above.

In summary, diatoms have the highest temperature specific growth rate and the highest sinking rate. Thus, diatoms are prevalent where the nutrient and light regime allow for growth rates sufficient to overcome losses by sinking. Chlorophytes and coccolithophores are transitional species in the model. Their nutrient and light requirements and lower sinking rates allow them to accumulate in regions where diatoms are unable to exploit the available nutrients. Cyanobacteria have low nutrient requirements and the lowest sinking rates which allow them to dominate in the central ocean gyres. However, the generally poor nutrient regimes in these regions prevent large accumulations of biomass.

The model phytoplankton groups and herbivores are initialized with a uniform distribution of 0.05 mg Chl m^{-3} while the two detrital pools are initialized at 0.0 mg Chl m^{-3}. The model nitrate and silicate fields are initialized with the annual mean fields of nitrate and silicate from the 1998 World Ocean Atlas (Conkright et al., 1998). Dissolved iron is initialized using the annual mean nitrate fields and the data of Fung et al. (2000) and ammonium is initialized at 0.5 μM. The coupled ice-ocean-biogeochemical model was integrated with the atmospheric forcing described above for 20 years. The model was then integrated for an additional 5 years, during which the monthly mean fields were saved. The results presented as a control experiment are the monthly mean fields averaged over the final 5 year integration.

2.3 High- and low-NAO phases Experiments

In addition to the control simulation discussed above, two further numerical experiments were carried out using the atmospheric forcing composited from years with high and low NAO index values. The biological component of these simulations remains the same as that of the control simulation; the high- and low-NAO runs differ only in the atmospheric forcing fields. Five years of a high-NAO index (1973, 1983, 1989, 1995 and 2000) and five years of a low-NAO index (1955, 1963, 1964, 1969 and 1996) (Fig. 1a) were selected and the atmospheric forcing fields of each five high- and low-NAO years were averaged. The composited atmospheric variables are sea level pressure, wind stress, air temperatures, specific humidity and wind speed. Relative to the average conditions in the northern North Atlantic, the NAO+ (NAO-) phase is characterized by stronger (weaker) heat loss, stronger (weaker) westerlies, deeper (shallower) mixed layers and colder (warmer) upper ocean temperatures.

Starting from the initial 20 year run of the control simulation, the NAO+ and NAO- cases were integrated for an additional 5 years, during which the monthly mean fields were saved. The results presented as the high and low NAO experiment are the monthly mean fields averaged over the final 5 year integration.

3 Results

3.1 Control Run

3.1.1 Area averaged chlorophyll

To validate the model results, we begin by examining the average monthly mean surface chlorophyll field from the control run compared to both satellite-derived (blended CZCS (Gregg and Conkright, 2001) and SeaWiFS) and *in situ* observation (O'Brien et al., 2002) in three sub-

basins of the Atlantic Ocean (Figure 2). In the North Atlantic sub-basin (Figure 2a), the control simulation shows a spring bloom beginning in April, with elevated chlorophyll levels extending into October. The peak bloom occurs in May and June, with average chlorophyll values reaching 1.00-1.20 mg Chl m^{-3}. Preceding and following this period, the average surface chlorophyll values fall to less than ~0.40 mg Chl m^{-3}. The time series of the monthly mean CZCS data also indicate a bloom in May-June and chlorophyll levels remain as high as 0.80 mg Chl m^{-3} continue until December. Except in May and June, the chlorophyll concentrations in the CZCS observations are approximately twice as high as in the control simulation. However, since CZCS data are generally sparse when the solar zenith angle is high, the area means are not representative of the true conditions during the winter months. In contrast to the control simulation and the CZCS observation, the SeaWiFS time series indicates an earlier spring bloom, which occurs in May and rapidly decreases by June (Gregg and Conkright, 2002). The seasonally averaged *in situ* observations are generally consistent with both the satellite-derived data and the control simulations at the peak bloom. However, the model underestimates the winter and fall values.

In the Central Atlantic sub-basin (Figure 2b), the model time series parallels the observations, ranging from 0.10 mg Chl m^{-3} to 0.25 mg Chl m^{-3}. Except for the *in situ* observations, the observational time series do not show strong a seasonal variability. The model shows the lowest chlorophyll values (~0.10 mg Chl m^{-3}) among all of the time series. In contrast, the *in situ* data indicate values greater than 0.30 mg Chl m^{-3} in winter and spring. While the surface chlorophyll values from the model appear much too weak in the Central Atlantic, the model does capture the seasonal trend in the satellite observations, with the lowest mean values in August and September and higher values in late winter and early spring.

In the Equatorial Atlantic sub-basin (Figure 2c), the model time series again shows a weak seasonal signal, whereas those in the observations indicate some seasonal variations. In particular, the time series from the SeaWiFS measurement reaches a peak chlorophyll concentration of ~0.50 mg Chl m^{-3} in August. In the model Equatorial Atlantic, the lack of nutrient fluxes from rivers (including the Amazon and the Congo) could partially explain the poor agreement in this region. Also, SeaWiFS ocean color values could be overestimated because of signal contamination by colored dissolved organic matter (CDOM) from river runoff.

3.1.2 Model-SeaWiFS comparison: spatial distribution of chlorophyll

While the area averages indicate that the model is simulating the overall chlorophyll biomass in the model domain reasonably well, observations also indicate a great deal of spatial heterogeneity in the surface chlorophyll fields. Figure 3 presents the surface chlorophyll fields from the control run in April, May and June when the area averages indicate North Atlantic undergoes the most rapid change in chlorophyll biomass. For comparison, the corresponding chlorophyll fields derived from SeaWiFS are also shown.

In April (Figure 3a), the model bloom in the North Atlantic is underway as observed north of about 40°N. The high chlorophyll values from Cape Cod to Newfoundland are well simulated and the bloom around the British Isles is initiated as in the SeaWiFS observations. In these nutrient rich regions, diatoms out-compete the other phytoplankton groups. Further south in the nutrient poor water on the northern flank of the subtropical gyre, the bloom consists of chlorophytes. The model captures well the region of increased chlorophyll off the west coast of Africa where coastal upwelling brings nutrients to the surface to promote growth. Most of the model subtropics show only low chlorophyll concentrations ($\leq$0.40 mg Chl m^{-3}), which vary

little over the next two months. The local chlorophyll maximum in the equatorial region is well developed.

By May (Figure 3b), the bloom in the North Atlantic has spread over most of the subpolar gyre from about 40W eastward. An intense bloom (chlorophyll biomass values exceeding ~5 mg Chl m^{-3}) is occurring on the southeast coast of Iceland while a second, smaller bloom is occurring in the Labrador Sea. Diatoms are again the most prevalent species, except for the region around Iceland where chlorophytes are the dominant species. While this is a region of relatively high nutrient abundance, it is also characterized by very shallow mixed layer depths through the year. In this region diatoms, which sink rapidly, are unable to remain suspended within the mixed layer and are thus disadvantaged in comparison to much more slowly sinking chlorophytes. In May, the path of the Gulf Stream is evident as a tongue of low chlorophyll biomass ($\leq$0.40 mg Chl m^{-3}) waters at about 40°N. The chlorophyll concentration in the equatorial region continues to increase as observed. By June (Figure 3c), the subpolar bloom extends to 70°N, with values greater than 0.8 mg Chl m^{-3} over much of the region. The area of the bloom dominated by diatoms retreats west as the silicate concentration drops, resulting in a species shift from diatoms to chlorophytes. The Labrador Sea remains dominated by diatoms.

As the previous discussion shows the comparison of model fields to the corresponding SeaWiFS observations is quite successful. However, there are a few deficiencies in the model: the coastal signals in the regions of major rivers are missing, the chlorophyll biomass is too low in the subtropical gyre and in the ice-covered regions of the subpolar gyre, and the model chlorophyll shows a meridional tilt across the top of the sub-tropical gyre. The first two areas of disagreement are related to the lack of lateral nutrient fluxes (primarily from river runoff). This leads to obvious deficits in chlorophyll biomass near major rivers such as the Amazon and

Congo Rivers, but as noted above, the SeaWiFS signal could also be contaminated by CDOM. Secondarily, nutrients are not advected along the flanks of the central gyres, leading to anomalously low chlorophyll biomass within the simulated central and equatorial Atlantic. In regions of seasonal sea ice, the large chlorophyll biomass deficits are most likely due to the lack of bio-geochemical processes in the model sea ice, particularly seeding of diatoms during the early spring melt. While we cannot fully explain the meridional tilt of the model bloom compared to the observations, a comparison of the simulated and observed isotherms (from Reynolds et al., 2002) (Figure 3) indicate that the major source of the meridional tilt is likely not the model ocean circulation itself. Rather, the strongly zonal nature of the observations leads us to believe that the discrepancy lies with the surface irradiance fields, which are used to force the model ecosystem.

3.2 High- and Low-NAO simulations

In section 3.1.1 we saw that there is a shift in the bloom peak between the CZCS and SeaWiFS chlorophyll time series in the North Atlantic region. As discussed in the introduction, the CZCS and SeaWiFS periods can be loosely characterized by positive and negative NAO phases. Although the SeaWiFS observations have occurred during a period of rising NAO index values, from strongly negative to moderately positive, the surface conditions have remained more typical of NAO- conditions. The SST variability as an area average in the northern North Atlantic (Fig. 1b) and SST difference between the CZCS and SeaWiFS period (Fig. 1c) show the striking difference between the 1980's and the latter 1990s.

Even though we cannot categorize the CZCS and particularly the SeaWiFS periods as representative of pure NAO+ or NAO- conditions, the oceanic conditions prevailing during these

observing periods are typical of the upper ocean response to the two phases of the NAO. Instead of qualifying the CZCS and SeaWiFS periods solely by NAO index, we focus here on the upper ocean conditions; during the two observing periods, these conditions are sufficiently different so as to be treated as two separate forcing regimes. We expect that the cold 1980s were a period of deep mixed layers and the warm latter 1990s were period of shallow mixed layers in the subpolar gyre. The deep mixed layers during the cold regime would provide a higher nutrient environment as deeper, nutrient rich waters are mixed into the surface layer. However, the colder surface temperatures would act as a brake on phytoplankton growth through the regulation of the intrinsic growth rate. In contrast, the warm regime case would provide for a faster phytoplankton growth rate but the lower nutrient abundance in the shallower mixed layers would limit overall phytoplankton biomass.

It should be noted that while there are also changes between the CZCS and SeaWiFS observations in the central and equatorial Atlantic (Figure 2b,c), the chlorophyll biomass in these regions appears to be strongly influenced by riverine inputs of nutrients. Since our model does not include these fluxes, we are unlikely to resolve the controlling mechanisms in the shift between CZCS and SeaWiFS in these regions. However, the northern North Atlantic bloom is strongly concentrated to the interior of the basin, and we anticipate that dynamic and thermodynamic conditions, and their effect on nutrient supply, are important for the changes in bloom timing. Therefore, in the discussion that follows, we limit our analysis to the region between 40°N and 70°N.

3.3 Low - High NAO Model Fields

The April difference fields (Low NAO - High NAO) for mixed layer depth, silicate and temperature are shown in Figure 4. As expected, the April mixed layer depths (Figure 4a) are much deeper over most of the subpolar North Atlantic in the NAO+ case while south of ~54°N the mixed layers are deeper in the NAO- case. The silicate difference fields in April (Figure 4b) confirm the expectation that the nutrient supply at the start of the bloom period should be enhanced where mixed layers are deeper. Thus, north of ~54°N, the silicate is lower in the NAO- case in regions where the mixed layer depths are shallower (Figure 4a). South of this latitude, the silicate concentrations in the NAO- case are generally higher, corresponding to regions where the mixed layers are deeper. The corresponding field for nitrate is similar to the silicate field (not shown). However, the control run indicates that the April-May bloom in the subpolar North Atlantic is largely composed of diatoms and that the region of diatom bloom is determined primarily by the extent of high silicate concentration. Temperature (Figure 4c) behaves in the opposite sense to silicate so that where mixed layers are shallower the temperature is warmer. Thus, the entire northern half of the North Atlantic shows a positive temperature difference and the southern region shows a negative temperature difference.

3.3.1 Chlorophyll variability in the North Atlantic sub-basin

If the shift in bloom time recorded by the CZCS and SeaWiFS observations are the result of cold and warm oceanic regimes, then we expect that the area averaged chlorophyll from the model NAO+ and NAO- simulations should reflect a similar shift in bloom timing. This scenario appears to be true (Figure 5a); the NAO+ simulation shows a peak bloom in June, coincident with CZCS, while the NAO- simulation blooms in May, coincident with SeaWiFS (1997-2002).

The 1998 SeaWiFS observation, when the NAO index was lowest of the observational period, also blooms in May. The shift in bloom between the NAO+ and NAO- cases arises from both a much stronger and earlier diatom bloom as well as increased May chlorophytes biomass in the NAO- case (Figure 5b).

The May Low NAO - High NAO difference fields for diatoms and chlorophytes (Figure 6) indicate that for both these species, the region of increased May biomass is the central North Atlantic. There is little signal in the Labrador Sea (although there may be a bias due to the use of monthly averages). The region where both diatoms and chlorophytes show stronger May blooms is not characterized by higher nutrients. In fact, though most of the North Atlantic shows lower silicate (and nitrate) abundance in the NAO- case as a result of shallower mixed layers, the May bloom is actually stronger in these regions. The early May bloom in fact appears to be controlled by the warmer surface temperatures (Figure 4c) in the NAO- case. The effect of temperature is highlighted based on data from simulated 'stations' as described in the following section.

3.3.2 Station data

While the monthly mean fields shown so far indicate that the timing of the bloom is controlled by the ocean surface temperature, the model phytoplankton grow and decay much faster (O(10days)) than the one-month time scale. Thus, the monthly averages do not indicate the exact timing of the bloom and it is possible that the use of the monthly mean fields distorts interpretation of the dynamics and characteristics of the spring bloom for the NAO+ and NAO- simulations. Therefore, four locations (stations) are chosen within the sub-polar gyre and the model behavior during the NAO- and NAO+ phases are traced using daily mean values. The

station locations are chosen to be representative of differing ocean regimes during the high and low NAO phases; the locations and identifiers of the four stations are indicated on Figure 6a.

Station A is located in the Labrador Sea, a region where the mixed layer depths are shallower in the NAO- simulation than in the NAO+ simulation (Figure 4a) resulting in a lower silicate concentration but warmer surface temperature in April (Figure 4b,c). The bloom event at Station A is relatively weak, reaching a maximum of between 0.80 and 1.00 mg Chl m^{-3} in the NAO+ and NAO- cases for both diatoms (Figure 7a) and chlorophytes (Figure 7b). The bloom peak for chlorophytes is in mid to late July at Station A and thus the weak signal seen in the May difference fields (Figure 6a) is due solely to the diatom bloom. While the April silicate is less abundant in the NAO- case, the diatom bloom occurs earlier and with slightly larger amplitude than in the NAO+ case. The surface temperature at Station A (Figure 7c) indicates that the NAO- case is approximately 1°C warmer than the NAO+ case in April, suggesting that the relatively warmer condition produces the earlier onset of the May diatom bloom.

Station B is located southeast of Iceland in a region characterized by April difference fields (Figure 4a-c) similar to that of Station A. At Station B, both the diatoms and the chlorophytes appear to have relatively strong signals in the May difference fields (Figure 6a,b). The station data however reveal that the bloom at Station B is actually dominated by chlorophytes (Figure 7a,b) in both the NAO- and NAO+ cases. While the bloom magnitude of the chlorophytes at Station B in the NAO+ case is actually greater than in the NAO- case (10.0 mg Chl m^{-3} *vs.* 8.0 mg Chl m^{-3}), the NAO+ bloom occurs over the months of May and June. Thus, in the NAO+ case, use of the monthly mean creates an artificially low May chlorophyte signal. The result is a strong signal in the May chlorophyte difference field. The NAO+ diatoms at Station B also bloom in late May and early June but at much lower magnitudes than in the

NAO- case. The splitting of the bloom in the NAO+ case, in addition to the very weak NAO+ diatom magnitude, results in a large signal in the May difference field. The underlying cause of the later NAO+ bloom is the same as at Station A; that is, the NAO+ bloom is delayed by the colder surface temperatures relative to the NAO- case.

Station C is located west of Ireland, in a region with a strong silicate deficit in the NAO- case (Figure 4b). The station data indicate that both diatoms and chlorophytes begin blooming in April (Figure 7a,b), with the peak bloom time for both species in late April or early May. In May, the diatom biomass at Station C is very similar in both the NAO+ and NAO- case (Figure 7a), leading to a relatively weak signal in the May diatom difference field (Figure 6a), despite the obvious shift in the diatom bloom seen in the station values. The May difference field for chlorophytes (Figure 6b), however, is not due to a timing shift but rather the increased biomass present in the NAO- case (Figure 7b). The primary importance of the surface temperature in regulating the bloom is indicated by the strength of the NAO- diatom bloom (Figure 7a) despite the low relative silicate at this location seen in the April difference field.

At Station D, the characteristics of the April difference fields are reversed from the previous three stations. That is, in the NAO- case the mixed layers are deeper, the silicate abundance is greater and the surface temperatures are colder than in the NAO+ case. At Station D, diatoms bloom in April in the NAO+ case while in the NAO- case a much stronger diatom bloom occurs both in April and May (Figure 7a), a reflection of the much higher silicate abundance in the NAO- simulation at this location. The chlorophyte bloom at Station D (Figure 7b) is much weaker than the diatom bloom but follows the same pattern of the NAO+ case preceding the NAO- case. At Station D, the signal in the May difference fields (Figure 6a) results from both temperature and nutrient effects. The warmer NAO+ surface temperatures lead to an

April diatom bloom which has already decayed by May while the enhanced silicate abundance leads to a large and sustained April-May bloom in the NAO- case.

In summary, all stations show the effect of temperature in bloom timing, but only one station, D, shows a significant change (~100%) in the bloom (diatoms+chlorophytes) magnitude. Moreover, the contrast in the model response between Stations A-C and D is useful in highlighting the relative roles of surface temperature and nutrient availability in the two NAO simulations. Stations A-C lie north of the subpolar front and Station D lies south of the front in the subtropical region; the model temperature response and nutrient abundances for the NAO- and NAO+ cases are opposite in these two regions. At the subtropical Station D, the cooler temperatures of NAO- case shift the bloom peak later, but its enhanced nutrient availability in the NAO- case propels a massive growth of diatoms. Thus, the subpolar front also serves as a biological front. To the north, nutrient abundances are high and relatively insensitive to atmospheric variability. To the south, nutrient abundances are lower and atmospheric variability has a much larger impact on the availability of nutrients.

4 Summary and conclusions

A coupled ocean/ice/ecosystem model of the North Atlantic and Arctic Oceans has been used to simulate the ecosystem response to climatological, NAO+ and NAO- atmospheric forcing regimes. Examination of the model control simulation indicated that the model captured the overall features and magnitude of the seasonal phytoplankton bloom in the northern North Atlantic when compared to both *in situ* and satellite observations. However, the lack of riverine inputs of nutrients reduced the overall confidence in the model in the Central and Equatorial regions of the model domain.

Model simulations using composite forcing fields from high and low NAO index years indicated that the model phytoplankton respond primarily to the ocean surface temperature fields. While springtime nutrient levels were higher (lower) in the NAO+ (NAO-) case, the effect of the colder (warmer) surface temperatures on the growth rate of the phytoplankton was found to be the controlling factor in determining the time of the spring bloom in the subpolar gyre. In the NAO- case, the warmer surface temperatures produced a May bloom, while in the NAO+ case the colder surface temperatures delayed the bloom until June. The temperature effect should be considered as an interannual time-scale impact on biomass. If NAO- conditions, i.e. shallow mixing continues extended for periods of time, nutrient limitation will eventually have an effect on the bloom amplitude. The results from NAO+ and NAO- simulations were found to be consistent with the satellite observations of both CZCS and SeaWiFS, which indicate a shift in the time of the bloom in the North Atlantic between May (SeaWiFS, warm, NAO-) and June (CZCS, cold, NAO+).

Our results support the conclusions of Edwards et al. (2001) based on continuous plankton recorder surveys. They emphasize the surface temperature regimes associated with NAO phases: NAO+ phase and warm SSTs are associated with the increased phytoplankton in the early 1990s around the British Isles. A similar relationship is evident in the model results for the North Sea where diatom concentrations are higher and SSTs are warmer in the NAO+ case. In addition, the relationship between zooplankton and NAO is found by Conversi et al (2001). They show that *Calanus finmarchicus* abundance in the Gulf of Maine between 1961 and 1991 was positively correlated with the NAO index. This is consistent with our model simulations, where the Gulf of Maine SST is warmer in the NAO+ case supporting higher concentration of chlorophytes in May and higher grazer concentrations in summer.

The model results also indicated that inclusion of both seeding by sea ice in the marginal ice zones and lateral nutrient fluxes coming from the rivers are needed to improve the model results. Numerical experiments with interannually varying forcing on the improved model will be used to further investigate the linkage between atmospheric forcing and ecosystem response within the entire Atlantic Ocean model domain.

Acknowledgments

This work was supported by funding from NASA HQ Ocean Biology and Biochemistry Program and Physical Oceanography Program.

References

Barton, A.D., C.H. Greene, B.C. Monger, and A.J. Pershing, 2003: The continuous plankton recorder survey and the North Atlantic Oscillation: Interannual- to multi-decadal scale patterns of phytoplankton variability in the North Atlantic Ocean, *Progress in Oceanography*, 58, 337-358.

Behrenfeld, M., J. T. Randerson, C. R. McClain, G. C. Feldman, S. O. Los, C., J. Tucker, P. G. Falkowski, C. B. Field, R. Frouin, W. E. Esaias, D. D. Kolber and N. H. Pollack, 2001: Biospheric primary production during an ENSO transition. *Science*, 291, 2594-2597.

Blumberg, A. F. and G. L. Mellor, 1987: A description of a three-dimensional coastal ocean circulation model. *Am. Geophys. Union*, pp.1-208.

Cayan, D. R., 1992: Latent and sensible heat flux anomalies over the northern oceans: The connection to monthly atmospheric circulation. *J. Clim.*, 5, 354-369.

Conkright, M., S. Levitus, T. O'Brien, T. Boyer, J. Antonov and C. Stephens, 1998: World Ocean Atlas 1998 CD-ROM Data Set Documentation. Tech. Rep. 15, International Report 16 pp. Silver Spring, MD.

Conversi, A., S. Piontkovski and S. Hameed, 2001: Seasonal and interannual dynamics of *Calanus finmarchicus* in the Gulf of Maine (Northeastern US shelf) with reference to the North Atlantic Oscillation. *Deep-Sea Res. II*, 48, 519-530.

Deser, C. and M. L. Blackmon, 1993: Surface Climate Variations over the North Atlantic Ocean during Winter: 1900-1989. *J. Clim.*, 6, 1743-1753.

Dickson, R. R., P. M. Kelly, J. M. Colebrook, W. S. Wooster and D. H. Cushing, 1988: North winds and production in the eastern North Atlantic. *J. Plankton Res.*, 10, 151-169.

Dickson, R. R., J. Lazier, J. Meincke, P. Rhines and J. Swift, 1996: Long-term coordinated changes in the convective activity of the North Atlantic. *Prog. Oceanog.*, 38, 241-295.

Dutkiewicz, S., M. Follows, J. Marshall and W. W. Gregg, 2001: Interannual variability of phytoplankton abundances in the North Atlantic. *Deep-Sea Res. II*, 48, 2323-2344.

Edwards, M., P. Reid, and B. Planque, 2001: Long-term and regional variability of phytoplankton biomass in the Northeast Atlantic (1960-1995), *ICES J. of Mar. Sci.*, 58, 39-49.

Follows M., and S. Dutkiewicz, 2002: Meteorological modulation of the North Atlantic spring bloom, *Deep-Sea Res. II,* 49, 321-344.

Fung, I. Y., I. T. S. K. Meyn, S. C. Doney, J. G. John and J. K. B. Bishop, 2000: iron supply and demand in the upper ocean. *Global Biogeochem. Cycles*, 14, 281-295.

Gregg, W. W., 2002: Tracking the SeaWiFS record with a coupled physical/biogeochemical/ radiative model of the global oceans. *Deep-Sea Res. II*, 49, 81-105.

Gregg, W. W. and M. E. Conkright, 2001: Global seasonal climatologies of ocean chlorophyll: blending in situ and satellite data for the CZCS era. *J. Geophy. Res.*, 106, 2499-2515.

Gregg, W. W. and M. E. Conkright, 2002: Decadal changes in global ocean chlorophyll. *Geophy. Res. Lett.*, 29 (15), 1730, doi:10.1029/2002GL014689.

Gregg, W. W., P. Ginoux, P. S. Schopf and N. W. Casey, 2003: Phytoplankton and Iron: Validation of a global three-dimensional ocean biogeochemical model. *Deep-Sea Res. II*, 50, 3143-3169, doi:10.1016/j.dsr2.2003.07.013.

Häkkinen, S., 2002: Freshening of the Labrador Sea waters in the 1990s: Another great salinity anomaly? *Geophy. Res. Lett.*, 29 (24), doi:10.1029/2002GL015243.

Häkkinen, S. and G. L. Mellor, 1992: Modeling the seasonal variability of the coupled arctic ice-ocean system. *J. Geophy. Res.*, 97, 20285-20304.

Häkkinen, S and P. Rhines, 2004: Decline in subpolar North Atlantic circulation in the 1990s. *Science* , 304 (5670), 555-559, doi:10.1126/science.1094917.

Hurrell, J. W., 1995: Decadal trends in the North Atlantic Oscillation: Regional temperatures and precipitation. *Science*, 269, 676-679.

Levitus, S., R. Burgett and T. P. Boyer, 1994: Salinity, NOAA Atlas NESDIS 3. *World Ocean Atlas*, 3, 1-99.

Marshall, J. and F. Schott, 1999: Open ocean convection: observations, theory, and models. *Reviews of Geophysics*, 37 (1), 1-64.

Mauritzen, C. and S. Häkkinen, 1997: Influence of sea ice on the thermohaline circulation in the Arctic-North Atlantic Ocean. *Geophy. Res. Lett.*, 24, 3257-3260.

Mellor, G. L. and T. Yamada, 1982: Development of a turbulence closure model for geophysical fluid problems. *Rev. Geophys.*, 20, 851-875.

O'Brien, T. D., P. P. Murphy, M. E. Conkright, T. P. Boyer, J. I. Antonov, O. K. Baranova, H. E. Garcia, R. Gelfeld, D. Johnson, R. A. Locarnini, I. Smolyar and C. Stephens, 2002: World Ocean Database 2001. NOAA Atlas NESDIS 48, 7.

Reid, P. C., M. Edwards, H. G. Hunt and A. J. Warner, 1998: Phytoplankton change in the North Atlantic. *Nature*, 391, 546.

Reynolds, R. W., N. A. Rayner, T. M. Smith, D. C. Stokes and W. Wang, 2002: An Improved In Situ and Satellite SST Analysis for Climate. *J. Clim.*, 15 (13), 1609-1625.

FIGURE CAPTIONS

Fig. 1 (a) The North Atlantic Oscillation (NAO) index (Hurrell, 1995). The NAO+ years (1973, 1983, 1989, 1995 and 2000) and the NAO- years (1955, 1963, 1964, 1969 and 1996) were composited to form the NAO+ and NAO- forcing used in this study. b) The winter (JFM) average sea surface temperature (°C) in the subpolar North Atlantic (70 °W to 10 °E , 40 °N to 70 °N) from Reynolds et al. (2002) and c) the April SST (°C) difference between the SeaWiFS (1997-2003) and CZCS (1979-1986) observing periods.

Fig. 2 The monthly mean surface chlorophyll concentration (mg Chl m^{-3}) in the control simulation for the a) North Atlantic (40°N to 70°N) b) Central Atlantic (10°N to 40°N) and c) Equatorial Atlantic (10°S to 10°N) model sub-basins. Also shown are the climatological monthlymean 1997-2003 SeaWiFS (□) and 1979-1986 CZCS (Δ) observations and the seasonal mean observations from the World Ocean Atlas 2001 (*).

Fig. 3 The monthly mean surface chlorophyll fields (mg Chl m^{-3}) and the 12°C – 20°C isotherms (solid lines, contour interval 2°C) for the model control simulation (top) during a) April b) May and c) June. The bottom panels show the monthly mean (1997-2003) SeaWiFS observations and the 12°C – 20°C isotherms from the 1971-2000 NOAA Optimum Interpolation SST (V2) dataset (Reynolds et al., 2002) during the same months.

Fig. 4. The April difference fields (NAO- simulation - NAO+ simulation) of the a) mixed layer depth (m), b) surface silicate concentration (μM) and c) surface temperature (°C). The locations of four stations (*), which are discussed later in the text, are shown for reference.

Fig. 5 The a) monthly mean surface chlorophyll (mg Chl m^{-3}) and b) the chlorophyll biomass (mg Chl m^{-3}) of the two dominant species in the North Atlantic sub-basin for the NAO- and

NAO+ model simulations. In a) the monthly mean 1997-2003 SeaWiFS, 1979-1986 CZCS and 1998 SeaWiFS observations are shown for comparison.

Fig. 6 The May difference fields (NAO- simulation - NAO+ simulation) of the surface a) diatom biomass b) chlorophyte biomass (mg Chl m^{-3}).

Fig. 7 The daily mean surface diatom (left), chlorophyte (center) concentrations (mg Chl m^{-3}) and (right) temperature (°C) for stations A, B, C, D (top to bottom, respectively) in the model domain for the NAO- and NAO+ simulations.

a)

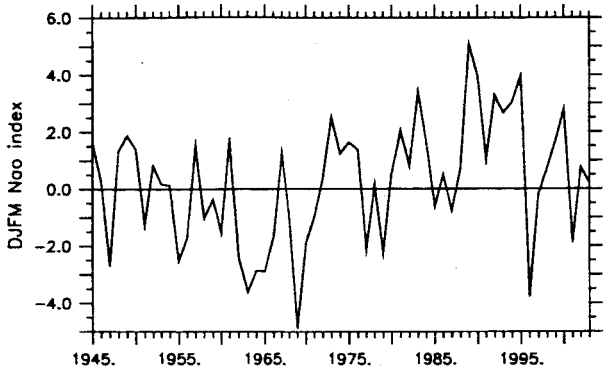
6.0
4.0
2.0
0.0
-2.0
-4.0
DJFM Nao index
1945.
1955.
1965.
1975.
1985.
1995.

b)

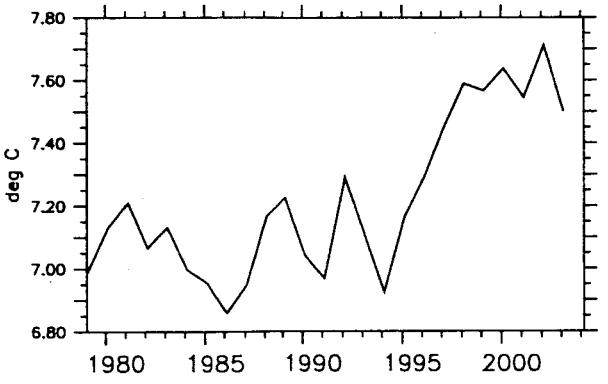
7.80
7.60
7.40
7.20
7.00
6.80
deg C
1980
1985
1990
1995
2000

c)

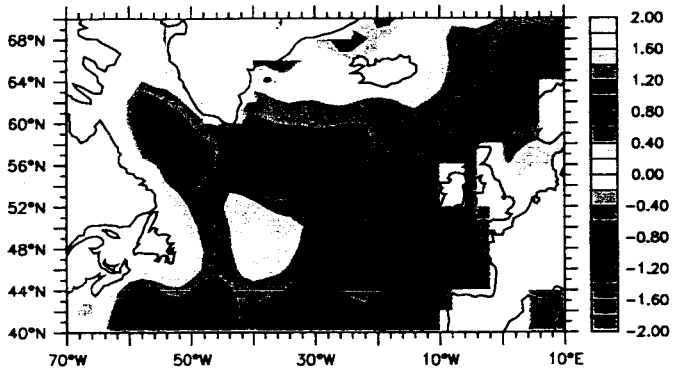
68°N
64°N
60°N
56°N
52°N
48°N
44°N
40°N
70°W
50°W
30°W
10°W
10°E
2.00
1.60
1.20
0.80
0.40
0.00
-0.40
-0.80
-1.20
-1.60
-2.00

Figure 1

a)

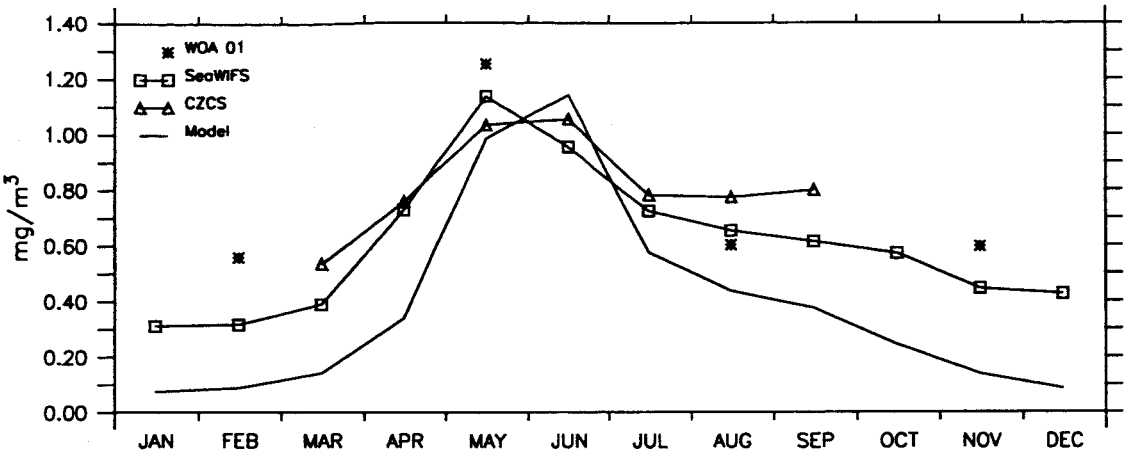
WOA 01
SeaWiFS
CZCS
Model
mg/m3
1.40
1.20
1.00
0.80
0.60
0.40
0.20
0.00
JAN
FEB
MAR
APR
MAY
JUN
JUL
AUG
SEP
OCT
NOV
DEC

b)

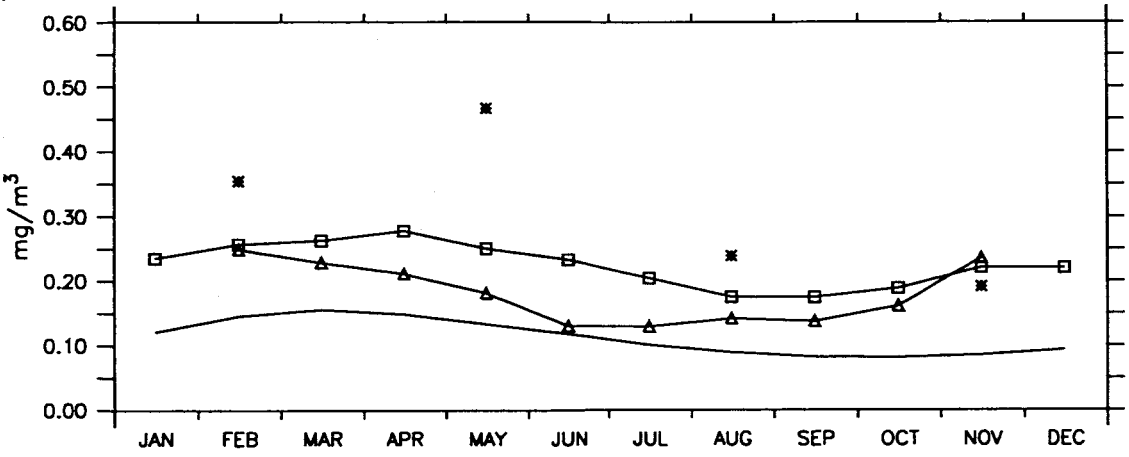
mg/m3
0.60
0.50
0.40
0.30
0.20
0.10
0.00
JAN
FEB
MAR
APR
MAY
JUN
JUL
AUG
SEP
OCT
NOV
DEC

c)

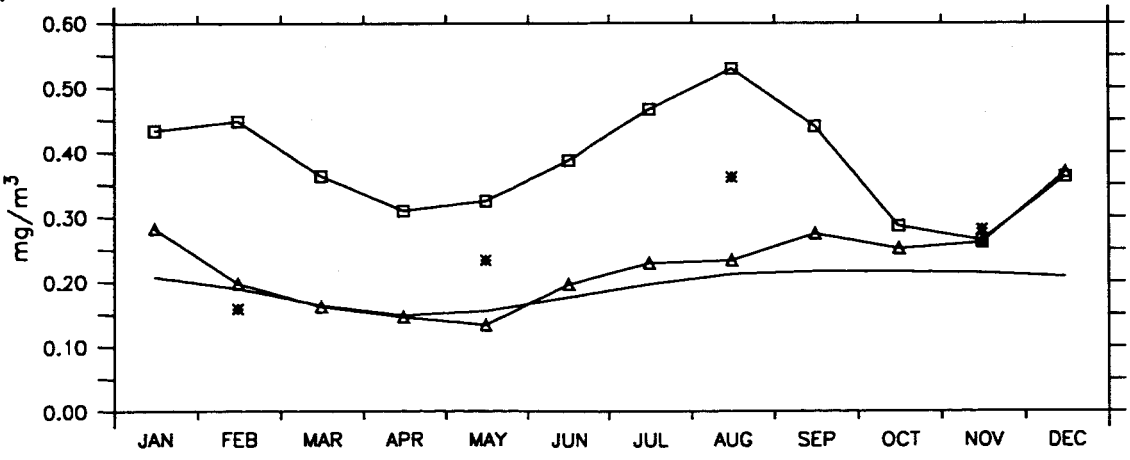
mg/m3
0.60
0.50
0.40
0.30
0.20
0.10
0.00
JAN
FEB
MAR
APR
MAY
JUN
JUL
AUG
SEP
OCT
NOV
DEC

Figure 2

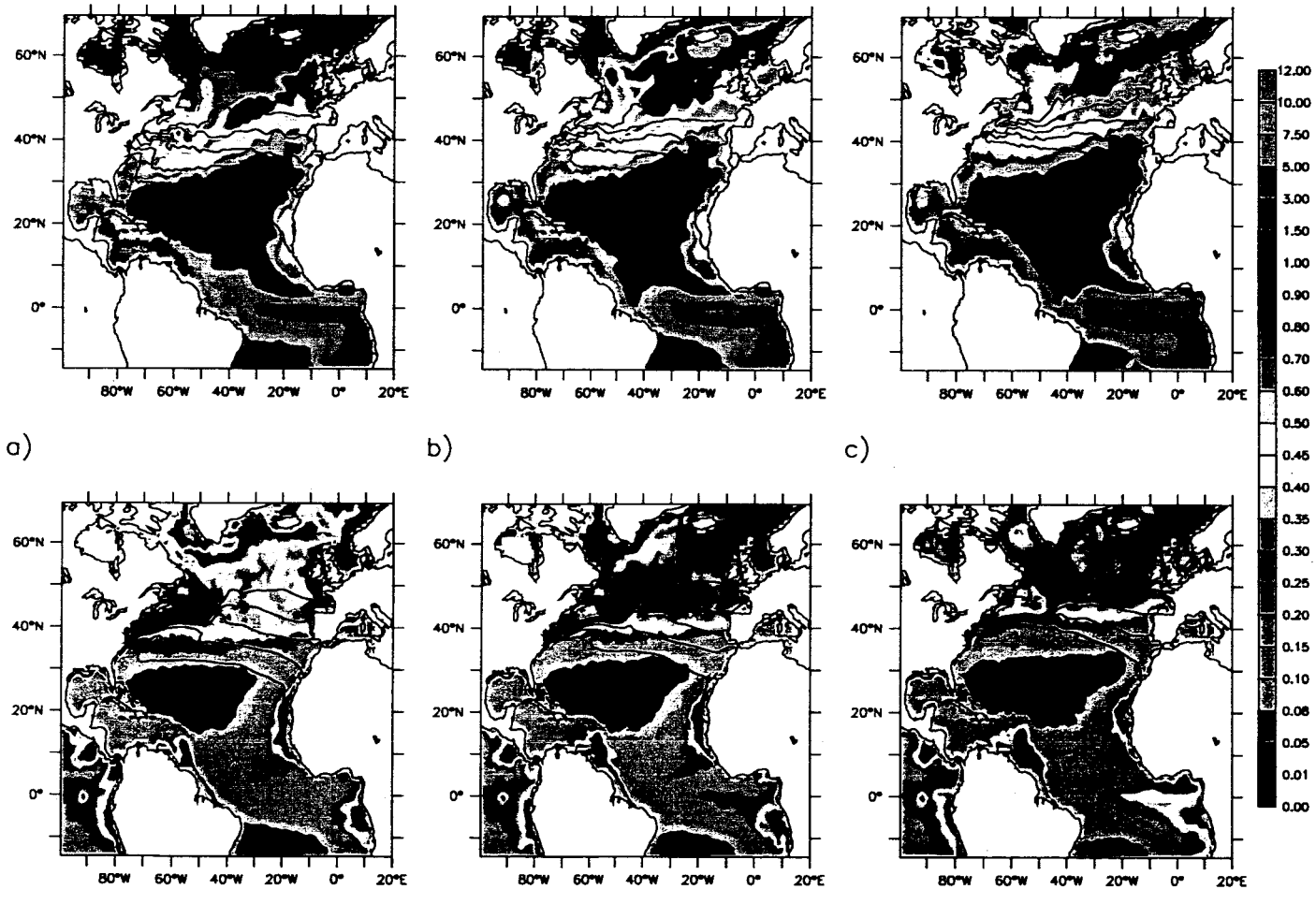
60°N
40°N
20°N
0°
80°W
60°W
40°W
20°W
0°
20°E
a)
b)
c)
12.00
10.00
7.50
5.00
3.00
1.50
1.00
0.90
0.80
0.70
0.60
0.50
0.45
0.40
0.35
0.30
0.25
0.20
0.15
0.10
0.08
0.05
0.01
0.00

Figure 3

a)

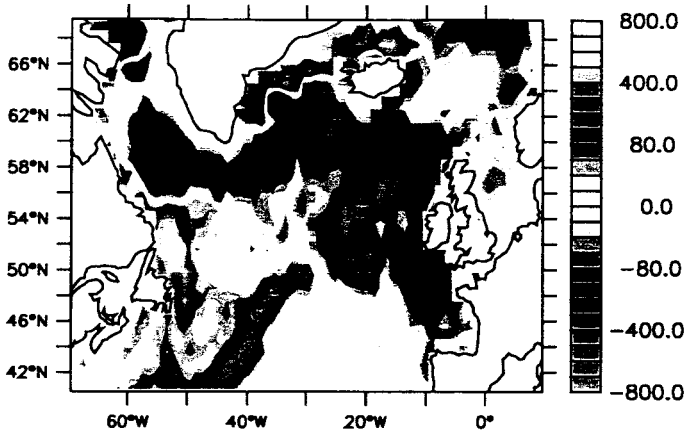
66°N
62°N
58°N
54°N
50°N
46°N
42°N
60°W
40°W
20°W
0°
800.0
400.0
80.0
0.0
-80.0
-400.0
-800.0

b)

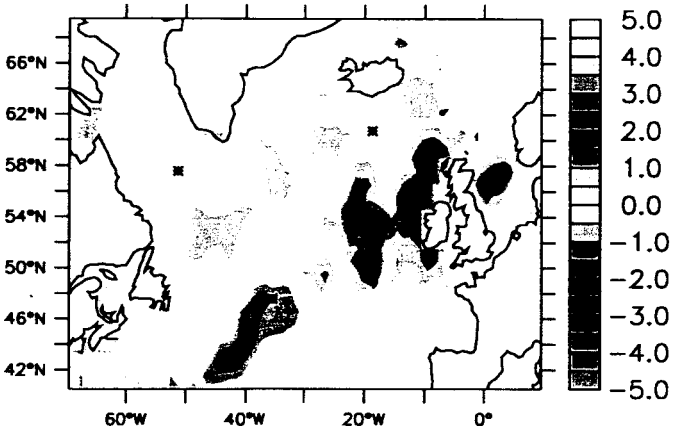
66°N
62°N
58°N
54°N
50°N
46°N
42°N
60°W
40°W
20°W
0°
5.0
4.0
3.0
2.0
1.0
0.0
-1.0
-2.0
-3.0
-4.0
-5.0

c)

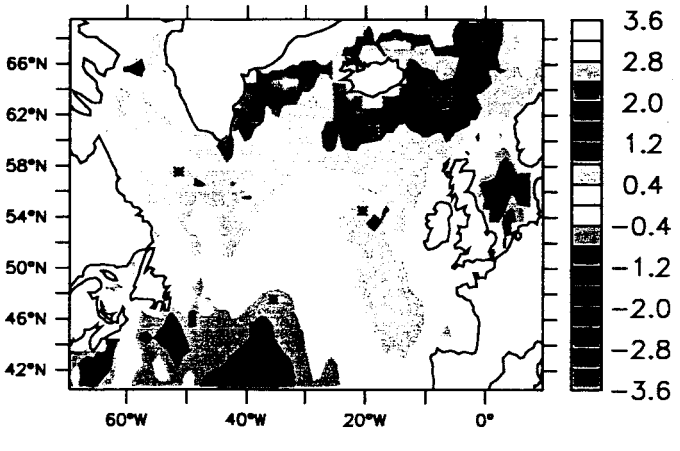
66°N
62°N
58°N
54°N
50°N
46°N
42°N
60°W
40°W
20°W
0°
3.6
2.8
2.0
1.2
0.4
-0.4
-1.2
-2.0
-2.8
-3.6

Figure 4

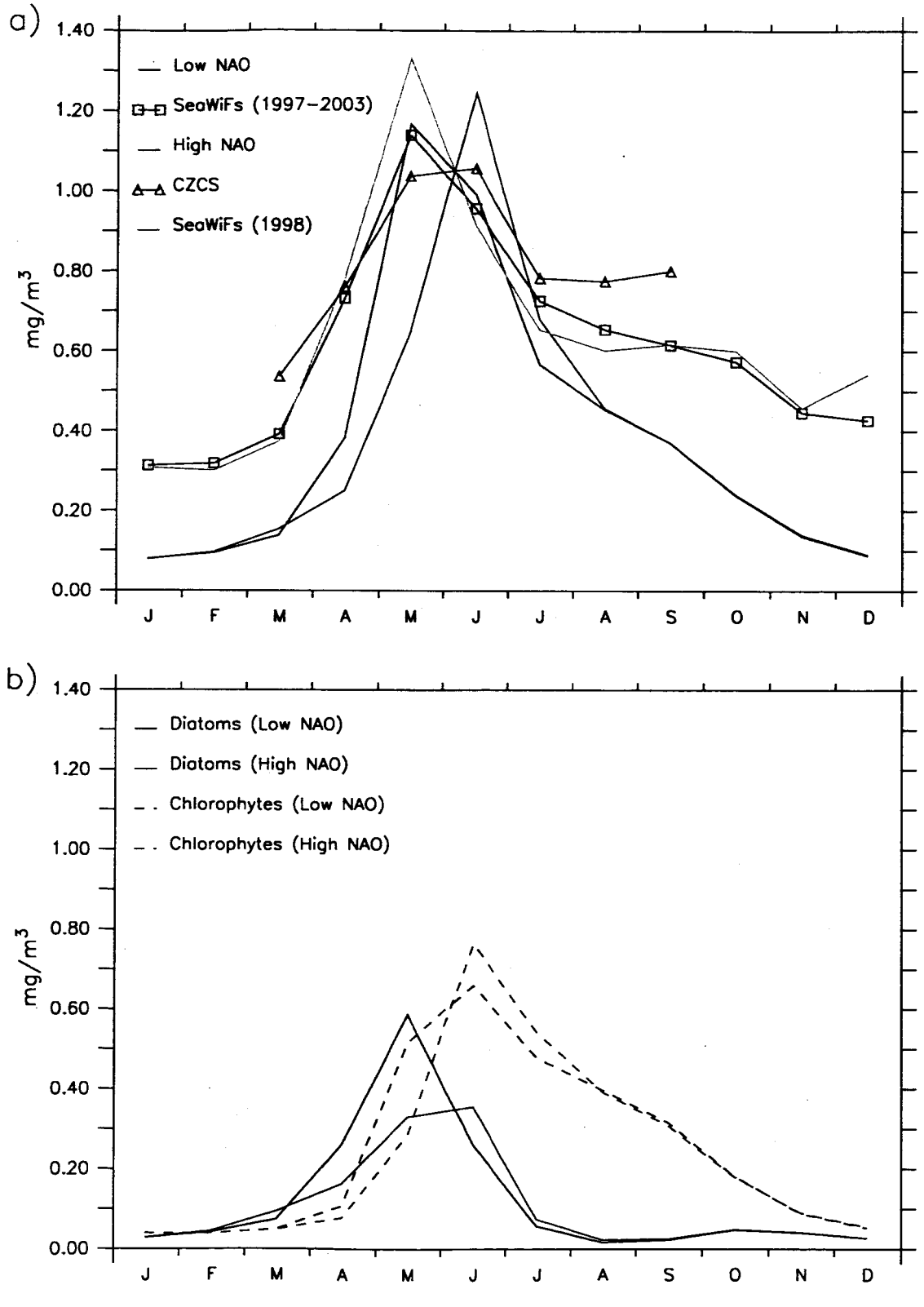
a)
Low NAO
SeaWiFs (1997–2003)
High NAO
CZCS
SeaWiFs (1998)
mg/m3
1.40
1.20
1.00
0.80
0.60
0.40
0.20
0.00
J F M A M J J A S O N D
b)
Diatoms (Low NAO)
Diatoms (High NAO)
Chlorophytes (Low NAO)
Chlorophytes (High NAO)
mg/m3
1.40
1.20
1.00
0.80
0.60
0.40
0.20
0.00
J F M A M J J A S O N D

Figure 5

a)

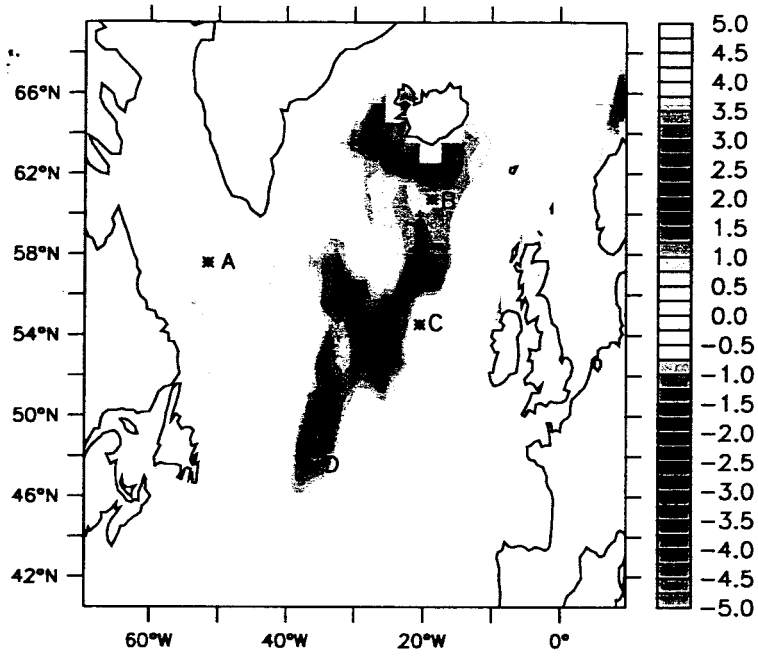
66°N
62°N
58°N
54°N
50°N
46°N
42°N
60°W
40°W
20°W
0°
A
B
C
D
5.0
4.5
4.0
3.5
3.0
2.5
2.0
1.5
1.0
0.5
0.0
−0.5
−1.0
−1.5
−2.0
−2.5
−3.0
−3.5
−4.0
−4.5
−5.0

b)

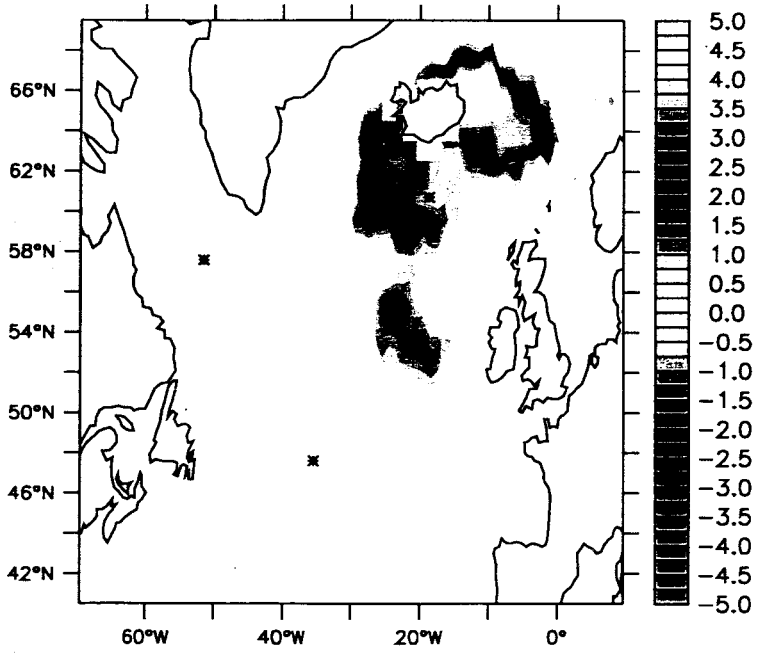
66°N
62°N
58°N
54°N
50°N
46°N
42°N
60°W
40°W
20°W
0°
5.0
4.5
4.0
3.5
3.0
2.5
2.0
1.5
1.0
0.5
0.0
−0.5
−1.0
−1.5
−2.0
−2.5
−3.0
−3.5
−4.0
−4.5
−5.0

Figure 6

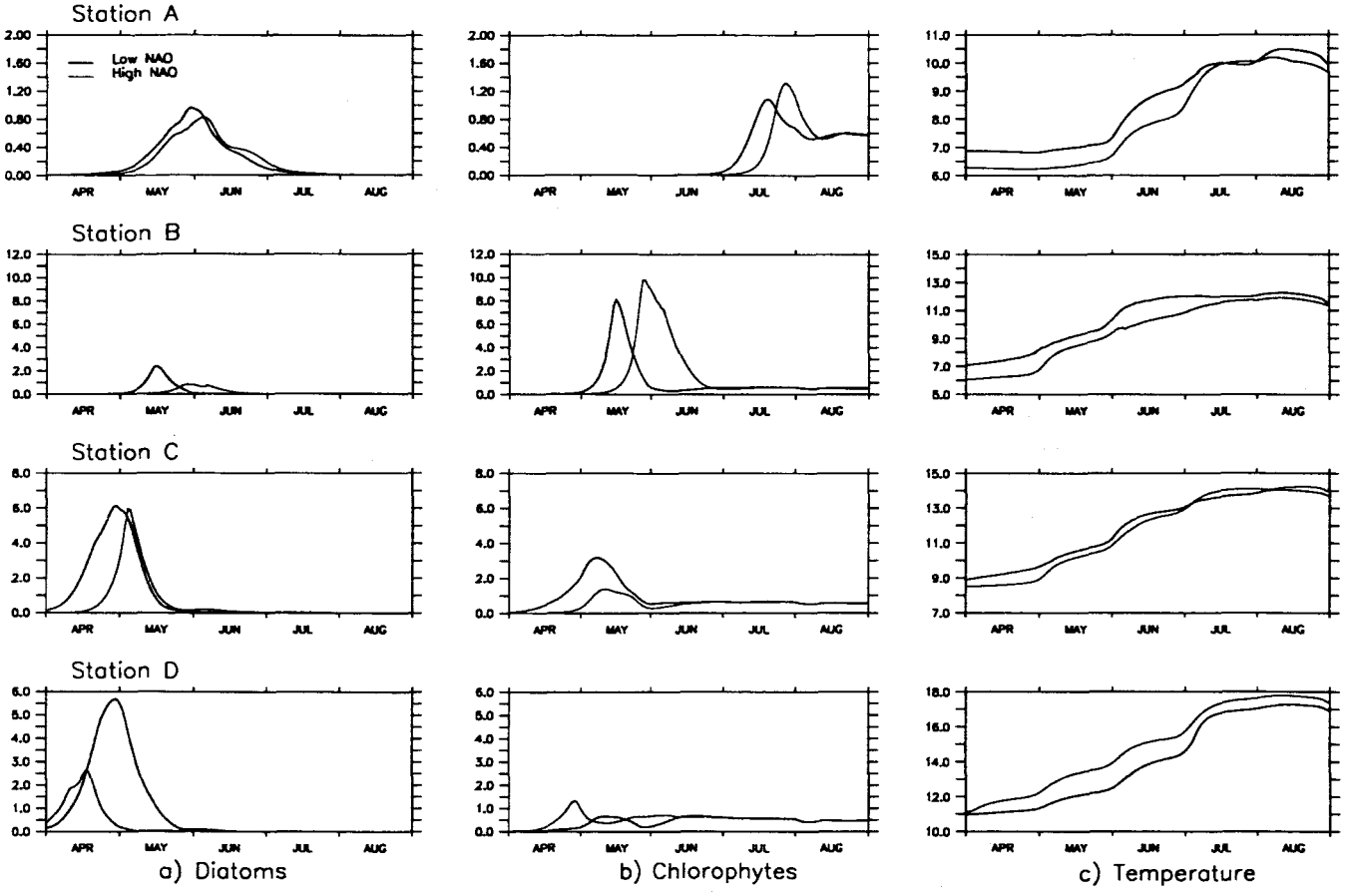
Station A
Low NAO
High NAO
Station B
Station C
Station D
APR
MAY
JUN
JUL
AUG
a) Diatoms
b) Chlorophytes
c) Temperature

Figure 7